Single-pole ladder at quarter filling

D. N. Aristov,[1,2,*] M. N. Kiselev,[3,4] and K. Kikoin[5]
[1]*Institut für Theorie der Kondensierten Materie, Universität Karlsruhe, 76128 Karlsruhe Germany*
[2]*Center for Functional Nanostructures, Universität Karlsruhe, 76128 Karlsruhe, Germany*
[3]*The Abdus Salam International Centre for Theoretical Physics, Strada Costiera 11, 34014 Trieste, Italy*
[4]*Material Science Division, Argonne National Laboratory, Argonne, Illinois 60439, USA*
[5]*School of Physics and Astronomy, Tel-Aviv University, Tel-Aviv 69978, Israel*
(Received 13 February 2007; published 7 June 2007)

We study the ground state and excitation spectrum of a quasi-one-dimensional system consisting of a pole and rungs oriented in opposite directions ("centipede ladder," CL) at quarter filling. The spin and charge excitation spectra are found in the limits of small and large longitudinal hoppings $t_{\|}$ compared to the on-rung hopping rate $t_{\perp}$ and exchange coupling $I_{\perp}$. At small $t_{\|}$, the system with ferromagnetic on-rung exchange demonstrates instability against dimerization. Coherent propagation of charge-transfer excitons is possible in this limit. At large $t_{\|}$, CL behaves like two-orbital Hubbard chain, but the gap opens in the charge excitation spectrum, thus reducing the symmetry from SU(4) to SU(2). The spin excitations are always gapless and their dispersion changes from quadratic magnonlike for ferromagnetic on-rung exchange to linear spinonlike for antiferromagnetic on-rung exchange in weak longitudinal hopping limit.

DOI: 10.1103/PhysRevB.75.224405 PACS number(s): 75.10.Pq, 71.10.Fd, 73.22.Gk

INTRODUCTION

The spin ladder systems attract much interest in both experimental and theoretical communities[1] during recent years. On the one hand, the ladder systems may be viewed as intermediate configuration between purely one-dimensional systems and periodic arrays of higher dimensions. On the other hand, in many cases, the simple theoretical models represent a good prototype for description of fundamental phenomena, such as metal-insulator transition, formation of various density wave states, low-dimensional superconductivity, and many other strongly correlated effects.[1] Besides, some of the toy theoretical models are simple enough to be solved exactly on the lattice or in the long-wave continuum limit.[2,3] The important experimental realizations of the ladder systems (see, e.g., Ref. 1) renewed an interest to imperfect spin chains and ladders affected by the chemical substitution, pressure, or radiation defects. Although the literature on symmetric two-leg ladders at half-filling is quite extensive,[1,2,4] not so much is known about the effects of strong asymmetry in the exchange interaction (or hopping) between the legs.[5] There are still many open questions about the doped two-leg ladders away from the half-filling regime.[6,7] Most of considered cases are related to so-called incommensurate filling where, in spite of strong Coulomb (Hubbard) interaction, the ground state of the ladder is metallic. On the contrary, at the commensurate filling (e.g., quarter filling) the Umklapp processes already open a gap in charge excitation spectrum for weak interaction.[8,9] These effects can be consistently treated by means of bosonization technique.[2,4,10]

In this paper, we consider a model characterized by a gap opened due to kinematic constraints even before any interactions are taken into account. This model, which we call a centipede ladder (CL) or single-pole ladder [see Figs. 1(a)–1(c)], can be visualized as the strongly asymmetric limit of the two-leg ladder [Fig. 1(b)], where the interaction along one of the two legs is negligibly small compared to both interactions along the main leg and the rung, e.g., due to spatial orientation of the rungs [see Figs. 1(a) and 1(b)].

The family of centipede ladder-type systems schematically presented in Fig. 1(a) was synthesized as a stable organic biradical crystal PNNNO.[11] The analysis of this geometry for the case of half-filling (two electrons on the rung with infinite on-site repulsion) has shown[12,13] that this model differs from the symmetric two-leg ladder. The half-filled case for the centipede ladder belongs to the specific class of universality, manifesting itself in in fractional scaling (2/3) of the spin gap $\Delta/J_{\|} \sim (|J_{\perp}|/|J_{\|}|)^{2/3}$, where $J_{\perp}$ and $J_{\|}$ are the on-rung and inter-rung exchange coupling constants, respectively. This scaling was attributed to existence of hidden dynamical symmetries associated with quantum nature of spin rotators formed at each rung of the ladder and should be contrasted with the integer scaling discovered for the symmetric two-leg ladders.[5] The corresponding model of highly asymmetric two-leg ladder, where the interaction between the spins residing at the end of neighboring rungs is zero, has been labeled as spin rotator chain model,[12] because it may be mapped onto an effective one-dimensional (1D) chain with

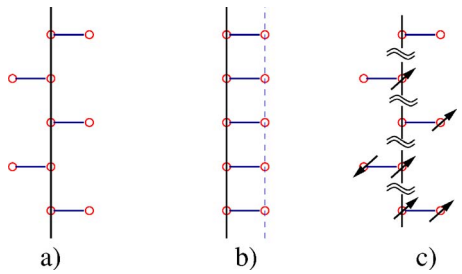

FIG. 1. (Color online) Centipede (a) and strongly asymmetric two-leg ladder (b). Several possible rung states (c) corresponding to vacancy, single occupied states, singlet and triplet states. Excited states with double on-site occupancy are not shown.

complicated on-site and intersite exchange interactions revealing "hidden" symmetries of spin rotator.

One may expect that the same geometry of centipede ladder away from the half-filling may also demonstrate a behavior very different from such for symmetric two-leg ladder and/or the partially filled chains. A quarter-filled CL is the next commensurate system where these differences should be looked for. At first sight, the quarter-filled CL, with strictly one electron per rung, is equivalent to the quarter-filled two-orbital Hubbard chain[14] (HC) with partially lifted orbital degeneracy. However, additional local symmetries related to the spin and charge degrees of freedom of electrons on a rung influence a structure of the ground state and the spectrum of low-energy excitation and makes the phase diagram of CL richer than that of half-filled HC or quarter-filled two-orbital HC. The aim of this paper is to reveal these other features. The phase diagram of CL promises to be complicated enough, and, in this paper, we confine ourselves with several limiting cases.

The paper is organized as follows: in Sec. I, we formulate the model and describe the hierarchy of the electronic states on the rung. Section II is devoted to analysis of the limit, where the on-rung ferromagnetic exchange is dominant. In Sec. III, we consider the case of weak longitudinal hopping for antiferromagnetic on-rung exchange. Section IV is devoted to the case of strong longitudinal hopping and discussion of various response functions at quarter filling. Details of calculations are presented in Appendix. In the last section, the summary of results and the perspectives are discussed.

I. MODEL AND HIERARCHY OF RUNG STATES

The generic model Hamiltonian is

$$\mathcal{H} = \mathcal{H}_r + \mathcal{H}_l, \tag{1}$$

where

$$\mathcal{H}_r = \sum_{si\sigma} \epsilon_s n_{si,\sigma} - t_\perp \sum_i (c^\dagger_{\alpha i,\sigma} c_{\beta i,\sigma} + \text{H.c.}) + \frac{1}{2}\sum_{si,\sigma} U n_{si,\sigma} n_{si,\bar{\sigma}} - I_\perp \sum_i \left(\mathbf{s}_{\alpha i}\mathbf{s}_{\beta i} - \frac{1}{4} n_{\alpha i} n_{\beta i} \right) \tag{2}$$

describes the electronic states on the rungs, and

$$\mathcal{H}_l = -\left(t_\parallel \sum_{i\sigma} c^\dagger_{\alpha i,\sigma} c_{\alpha i+1,\sigma} + \text{H.c.} \right) \tag{3}$$

is related to the longitudinal electron hopping along the leg. Here, $s=\alpha,\beta$ enumerates sites belonging to the leg (α) and the branch (β) in a given rung i. Without losing the generality, we assume the different surroundings $\epsilon_\alpha \neq \epsilon_\beta$ for the sites α,β. This condition can be equivalently rewritten in terms of two different electrochemical potentials: $\epsilon_{\alpha(\beta)} = \epsilon_0 \mp \mu$ with $\mu \neq 0$. The 1/4 filling is ensured by particular choice of the chemical potential μ.

The Hamiltonian (1) can be viewed as an extension of the spin rotator chain (SRC) model considered in Refs. 12 and 13 for the case of arbitrary electron filling. More precisely, the SRC model is characterized by single-pole geometry, Fig. 1(a), with exactly one electron per site; hopping is not allowed and only magnetic exchange between different spins is involved. In fact, that SRC model can be obtained from Eq. (1) for a half-filled case, i.e., one electron per site, in the limit $U \to \infty$. In that case, the usual reasoning leads to a conclusion that the direct hopping becomes forbidden, but it may generate the indirect (antiferromagnetic) exchange couplings $J_{\parallel(\perp)} \sim t^2_{\parallel(\perp)}/U$ within a given rung, $J_\perp$, and between neighboring rungs, $J_\parallel$. In the present study of quarter-filled case, we have to distinguish between the direct exchange $I_\perp$ (which is always physically present and can be of ferromagnetic sign) and the indirect exchange induced by $t_{\parallel(\perp)}$. For simplicity, we omit the direct longitudinal exchange $I_\parallel$ from the Hamiltonian because its inclusion does not alter the effects discussed below. We consider both the case of ferromagnetic on-rung coupling ($I_\perp > 0$), studied in (Refs. 12 and 13) for a half-filled single pole ladder, and the case of antiferromagnetic exchange ($I_\perp < 0$). Both the ground states and the excitation spectra are radically different in these two latter cases.

It is natural to use a single rung basis for characterization of the energy spectrum of single-pole ladder, Eq. (1). The set $\mathbb{S}$ of 16 rung basis states consists of an empty state $|0\rangle$ (which we will call a vacancy), four singly occupied rung states $|1,\alpha i\sigma\rangle = c^\dagger_{\alpha i\sigma}|0\rangle$, four doubly occupied rung states, which are split into singlet and/or triplet configurations, two doubly occupied on-site states, four triply occupied states, and a fully occupied state with four electrons. In the limit of strong Hubbard repulsion, $U \gg t_\parallel$, the lowest states on the rung i belonging to the charge sector $N_i=2$ (doubly occupied rungs) are

$$|2S,i\rangle = \frac{1}{\sqrt{2}}(c^\dagger_{\alpha i\uparrow} c^\dagger_{\beta i\downarrow} - c^\dagger_{\alpha i\downarrow} c^\dagger_{\beta i\uparrow})|0\rangle,$$

$$|2T1,i\rangle = c^\dagger_{\alpha i,\uparrow} c^\dagger_{\beta i,\uparrow}|0\rangle,$$

$$|2T0,i\rangle = \frac{1}{\sqrt{2}}(c^\dagger_{\alpha i\uparrow} c^\dagger_{\beta i\downarrow} + c^\dagger_{\alpha i\downarrow} c^\dagger_{\beta i\uparrow})|0\rangle,$$

$$|2T\bar{1},i\rangle = c^\dagger_{\alpha i,\downarrow} c^\dagger_{\beta i,\downarrow}|0\rangle. \tag{4}$$

Here, the quantum numbers of two-electron states are qualified as a singlet $2S$ and triplet $2T\lambda$ with $\lambda = 1, 0, \bar{1}$.

The energies corresponding to the eigenstates (4) are defined as follows:

$$E_{1,li} = \epsilon_0, \quad E_{2S,i} = 2\epsilon_0 - j, \quad E_{2Ti} = 2\epsilon_0 - I_\perp, \tag{5}$$

where $|\epsilon_0|$ is a single-electron ionization energy, and $j = 2t^2_\perp/U$ is the indirect exchange of spins at adjacent sites, which stems from virtual transitions including double occupancy. Strong Hubbard repulsion effectively excludes all states beyond the four states (4) in the low-energy part of the excitation spectrum with $N_i \geqslant 2$ (see below).

In a charge sector $N_i=1$, the electron spectrum demands further diagonalization. The states on a given rung are characterized by spin and pseudospin. Spin $\mathbf{s}_i$ is defined as usual, and pseudospin $\boldsymbol{\tau}_i$ is introduced as

$$\tau_i^z = \frac{1}{2}\sum_\sigma (n_{\alpha i\sigma} - n_{\beta i\sigma}), \quad \tau_i^x = \frac{1}{2}\sum_\sigma [c^\dagger_{\beta i\sigma} c_{\alpha i\sigma} + \text{H.c.}]. \quad (6)$$

The kinetic-energy term in Eq. (2) corresponding to the hopping along the rung may be cast in the form

$$\mathcal{K}_\perp = -2t_\perp \sum_i \tau_i^x, \quad (7)$$

while, assuming two different electrochemical potentials ϵ_α and ϵ_β, we get one more term

$$\mathcal{K}_{cp} = \sum_i \tau_i^z(\epsilon_\alpha - \epsilon_\beta) + \frac{1}{2}\sum_i N_i(\epsilon_\alpha + \epsilon_\beta) = -\mu\sum_i \tau_i^z + \epsilon_0 \sum_i N_i \quad (8)$$

in $\mathcal{H}_r$. Here, $N_i = n_{i\alpha} + n_{i\beta}$. Terms in Eqs. (7) and (8) proportional to τ^x and τ^z correspond to external uniform "magnetic" field, causing the Zeeman splitting of the rung orbital states. We discuss the formation of the orbital gap in the Sec. IV, taking everywhere below $\epsilon_\alpha = \epsilon_\beta$.

If the sites α and β are equivalent, the nondiagonal transitions described by τ_i^x are eliminated in the local basis of the bonding (+) and antibonding (−) states introduced in accordance with

$$|\pm, \sigma, i\rangle = \frac{1}{\sqrt{2}}(|1, \alpha i\sigma\rangle \pm |1, \beta i\sigma\rangle). \quad (9)$$

At finite $t_\perp$, this basis still diagonalizes the rung Hamiltonian and the corresponding single-electron energy levels are $\epsilon_\pm = \epsilon_0 \mp t_\perp$. One should stress that the doubly occupied states cannot be viewed as two bonding and/or antibonding orbitals on a rung, due to strong Hubbard repulsion, and the charge sector $N_i = 2$ is represented by the states (4). This is a specific property of CL in comparison with the two-orbital HC.

Another remarkable property of CL, which, in fact, allows double occupation of a rung without paying large energy U, is its instability against chain dimerization under certain conditions. To describe this instability, one should introduce the elementary cell for a CL with doubled lattice period. Such cell is occupied by two electrons, and its energy spectrum at zero $t_\parallel$ is easily found. The low-energy subset is formed by the dimerized states and the states with singly occupied rungs, respectively:

$$\{N_i = 2, N_{i\pm1} = 0\} = \{|2T\lambda, i; 0, i+1\rangle, |2S, i; 0, i+1\rangle\},$$

$$\{N_i = 1, N_{i+1} = 1\} = \{|\pm, \sigma, i; \pm, \sigma', i+1\rangle\}. \quad (10)$$

The corresponding two-electron energy levels are

$$E_T(2,0) = 2\epsilon_0 - I_\perp,$$

$$E_S(2,0) = 2\epsilon_0 - j,$$

$$E_{++}(1,1) = 2(\epsilon_0 - t_\perp),$$

$$E_{+-}(1,1) = 2\epsilon_0,$$

$$E_{--}(1,1) = 2(\epsilon_0 + t_\perp). \quad (11)$$

One concludes from Eq. (11) that the lowest-energy levels, which predetermine the spectrum of quarter-filled CL, are $E_T(2,0), E_S(2,0), E_{++}(1,1), E_{+-}(1,1)$. If $I_\perp < 2t_\perp$, the lowest two-electron states of this elementary cell belong to the subset $\mathbb{S}_h = \{+, \sigma, i; +, \sigma', i+1\}$ with one bonding orbital per rung. In the opposite case $I_\perp > 2t_\perp$, the lowest state corresponds to (2,0) occupation of adjacent rungs. We denote the corresponding subset as $\mathbb{S}_d = \{2T, 2S, i; 0, i+1\}$. At finite longitudinal hopping, CL forms homogeneous quarter-filled chain in the former case and dimerized chain with alternating (2,0) occupation in the latter case.

In the case of negative (antiferromagnetic) exchange $I_\perp$, the ground state is homogeneous quarter-filled chain belonging to the subset $\mathbb{S}_h = \{+, \sigma, i; +, \sigma', i+1\}$ and the lowest excited state is E_S [see Fig. 2(b)].

In the following two sections, we discuss charge and spin excitation spectra of CL in the limit of weak longitudinal hopping. Looking at Figs. 2(a) and 2(b) and Eqs. (11), we see that in case (a), one may find a regime, where only the levels E_{++} and E_T are involved in formation of the low-energy excitations, whereas in case (b), at least three states E_{++}, E_S, E_{+-} are involved.

II. WEAK LONGITUDINAL HOPPING LIMIT, FERROMAGNETIC ON-RUNG EXCHANGE

In this section, we analyze the quarter-filled CL with $I_\perp > 0$ in a situation where the longitudinal hopping is small in comparison with the on-rung coupling constants, and the inequalities

$$I_\perp > 2t_\perp, \quad t_\parallel \ll I_\perp - 2t_\perp \quad (12)$$

are valid. In the absence of longitudinal hopping, each second rung is empty and all doubly occupied rungs are in spin-one triplet states [see Fig. 2(a)]. One has to study longitudinal spin and charge excitations at finite $t_\parallel$ above the dimerized ground state with alternating rungs $\ldots|2T\lambda, i\rangle, |0, i+1\rangle\ldots$. The charge excitations arise due to transitions $\mathbb{S}_d \Leftrightarrow \mathbb{S}_h$. These excitations (charge-transfer excitons) are obviously gapped, so that the low-energy excitations belong to the spin sector.

In zeroth-order approximation, the spectrum of rung dimers is determined by the eigenstates of the Hamiltonian (2) in a charge sector $N_i = 2$ for ferromagnetic on-rung exchange. These dimers are in the state of *spin rotator*,[12,13,15] characterized by the singlet-triplet manifold $\{|2T\lambda, i\rangle, |2S, i\rangle\}$, with the energy gap between two spin states given by

$$\Delta E_{ST} = I_\perp - j. \quad (13)$$

Longitudinal hopping (3) generates indirect exchange produced by the electron cotunneling via empty odd rungs. To derive the corresponding spin Hamiltonian, we have to exclude the charge sector $\mathbb{S}_h$ from the effective phase space. It is seen from Fig. 2(a), that the singlet states are effectively quenched at the energy scale $I_\perp - 2t_\perp$, which characterizes the charge-transfer gap, so that one may confine oneself with the subspace $\{\mathbb{S}'_d, \mathbb{S}_h\}$, with singlet states excluded from the subset $\mathbb{S}'_d = \{2T, i; 0, i+1\}$ of "polar" states.

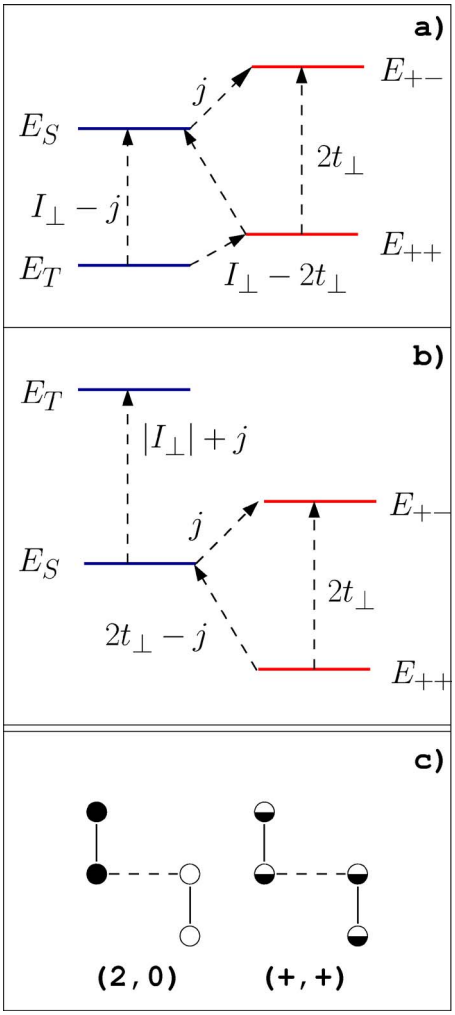

FIG. 2. (Color online) Two-electron level structure for two neighboring rungs. (a) Ferromagnetic on-rung exchange. The ground state is dimerized. (b) Antiferromagnetic on-rung exchange. The ground state is array of bonding orbitals. (c) Occupation scheme for two different ground states: filled, empty, and half-filled circles correspond to occupied (triplet), empty (vacancy), and bonding electron states, respectively. Transitions within a given charge spin or charge sector and transitions between different sectors are marked by vertical and slanting dashed arrows, respectively. The energies of these transitions are also shown. The two-electron energy levels for singlet (E_S), triplet (E_T) bonding-bonding (E_{++}), and bonding-antibonding (E_{+-}) states are given in Eq. (11).

The remarkable property of the state S'_d is that the macroscopic configurational degeneracy of the Hubbard model with partial filling is removed due to dimerization. The only remaining even-odd degeneracy of the dimerized ground state of zero-order Hamiltonian may be also removed in the case of CL with odd number of rungs $M=2N+1$, where, say, all even rungs $0,2,\ldots,2N$ are doubly occupied and all odd rungs $1,3,\ldots,2N-1$ are empty. Then only the trivial spin degeneracy remains, and one may strictly define the effective exchange Hamiltonian in the fourth-order of Brillouin-Wigner expansion

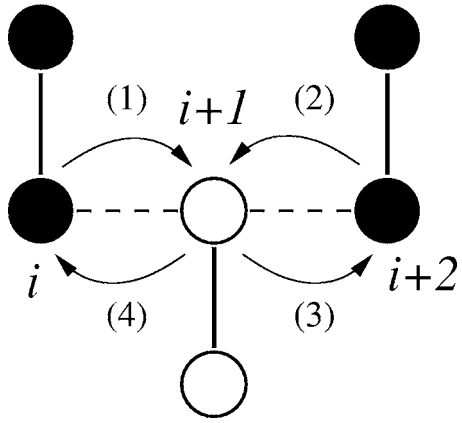

FIG. 3. Scheme of superexchange induced in fourth-order hopping processes in dimerized CL. Arrows indicate sequential electron hops resulting in the intermediate states (16). Notations for the occupation scheme are the same as for Fig. 2(c).

$$\mathcal{H}_{eff} = \mathcal{H}_r + \langle \Psi_0 | \mathcal{H}_l^{(4)} | \Psi_0 \rangle, \tag{14}$$

where the brackets $\langle \Psi_0 | \cdots | \Psi_0 \rangle$ stand for the dimerized polar ground state with alternating triplet spin states and vacancy states

$$\mathcal{H}_l^{(4)} = \frac{\mathcal{H}_l |\phi^{(1)}\rangle\langle\phi^{(1)}| \mathcal{H}_l |\phi^{(2)}\rangle\langle\phi^{(2)}| \mathcal{H}_l |\phi^{(3)}\rangle\langle\phi^{(3)}| \mathcal{H}_l}{(-E_0^{(1)})(-E_0^{(2)})(-E_0^{(3)})}. \tag{15}$$

Here, the projection operators

$$P^{(\alpha)} = |\phi^{(\alpha)}\rangle\langle\phi^{(\alpha)}|, \quad \alpha = 1,2,3$$

include the states which are generated from the ground state $|\Psi_0\rangle$ after first, second, and third actions of the operator $\mathcal{H}_l$, respectively, and $E_0^{(\alpha)}$ are the corresponding excitation energies. The fourth-order cotunneling process resulting in effective kinematic exchange is illustrated by Fig. 3. It is evident that only the clusters $(i, i+1, i\pm 2)$ are involved in formation of the effective exchange Hamiltonian, where i stands for any even site. We consider here the simplest situation, where the singlet intermediate states can be discarded in the main order, which happens at $t_\parallel/(I_\perp - j) \ll t_\parallel/(I_\perp - 2t_\perp)$. This simplification does not change our qualitative conclusions.

$$|\phi^{(1)}\rangle = |+\sigma_1, i; +\sigma_2, i+1; 2T\lambda, i+2\rangle,$$

$$|\phi^{(2)}\rangle = |+\sigma_1, i; 2T\lambda_1, i+1; +\sigma_3, i+2\rangle,$$

$$|\phi^{(3)}\rangle = |+\sigma_1, i; +\sigma_4, i+1; 2T\lambda', i+2\rangle. \tag{16}$$

It is seen from Eq. (16) and Fig. 3 that the intermediate states involve electron cotunneling exchange between two nearest even sites with formation of a virtual doubly occupied triplet state on the odd site between them. This mechanism is known as superexchange in the theory of magnetic dielectrics. Appearance of intermediate triplet states $|2T\lambda\rangle$ in the indirect exchange interaction is the peculiarity of CL: unlike the two-orbital HC model, double occupation of intermediate state does not cost the Hubbard repulsion energy U,

because the two electrons on a rung may occupy different sites. As a result, we come to the following effective spin Hamiltonian:

$$\mathcal{H}_{eff} = \mathcal{H}_r - J_{\parallel} \sum_i \mathbf{S}_i \cdot \mathbf{S}_{i+2}, \tag{17}$$

where the site index i stands only for even rungs of CL. The coupling constant is

$$J_{\parallel} = \frac{t_{\parallel}^4}{16\Delta_T^3}, \tag{18}$$

where $\Delta_T = I_{\perp} - 2t_{\perp}$ is the charge-transfer energy gap [see Fig. 2(a)]. The details of calculation are provided in Appendix. Deriving [Eq. (18)], we assumed that the singlet state does not contribute to superexchange. This assumption holds provided $\Delta_T \ll \Delta E_{ST}$.

Thus, we have demonstrated that the problem of quarter-filled CL is mapped onto the familiar problem of spin-one Heisenberg chain with ferromagnetic exchange in the limit of weak longitudinal hopping under conditions (12). Only the even sites are involved in formation of the gapless spin excitations, which, apparently, may be described in terms of the spin-wave theory.[16]

As to the charge-transfer excitons, $|+\sigma, i; +\sigma', i+1\rangle$, shown in the right column of Fig. 2(c), these states, like other excitons, can exist both in triplet and singlet spin configurations. These excitations may propagate coherently, and the dispersion law for coherent propagation mode is predetermined by the fourth-order cotunneling processes similar to those responsible for the indirect exchange described by Eqs. (15) and (16). To provide translation of such exciton from one cell of dimerized CL to another, two electrons should hop to the right $(i \to i+1; i+1 \to i+2)$ and then to the left $(i+2 \to i+1; i+3 \to i+2)$. This fourth-order indirect "exchange" provides excitons with the dispersion law $\omega_q \sim \Delta_T + 2J_{\parallel} \cos 2qa$, where a is the lattice spacing along the leg.

Thus, we have shown, in this section, that the spin excitations in the CL with ferromagnetic on-rung exchange are gapless magnonlike modes, whereas the excitations in a charge sector are gapped excitons describing coherent propagation of two bonding states along the chain.

III. WEAK LONGITUDINAL HOPPING LIMIT, ANTIFERROMAGNETIC ON-RUNG EXCHANGE

In the case of negative on-rung exchange hopping along the leg and small $t_{\parallel}$, so that the inequality

$$t_{\parallel} \ll 2t_{\perp} - j \tag{19}$$

is satisfied, the energy levels are ordered in accordance with Fig. 2(b), and the ground-state wave function of quarter-filled CL is given by the product of bonding orbitals

$$|\Psi_0\rangle = |\cdots + \sigma_i, i; + \sigma_{i+1}, i+1; + \sigma_{i+2}, i+2; \cdots\rangle. \tag{20}$$

In this sector of phase diagram, the quarter-filled CL is close in a sense to the quarter-filled two-orbital Hubbard chain (HC),[14] with lifted orbital degeneracy: each rung is occupied by one electron with bonding orbital, and the empty anti-

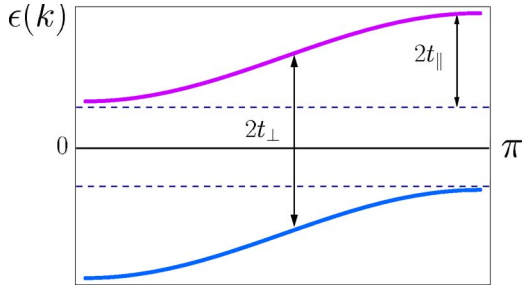

FIG. 4. (Color online) Tight-binding band structure for quarter-filled centipede model at $t_{\parallel} \ll t_{\perp}$. The occupied and empty orbital subbands $\epsilon_{\pm}(k)$ are shown. The chemical potential is chosen as a reference energy level.

bonding level is separated from this band by the orbital gap $\sim 2t_{\perp}$ [see Eqs. (7) and (8) and Fig. 4].

The important distinction from two-orbital HC roots in the structure of the doubly occupied states. Since two electrons on a rung occupy different orbitals in accordance with Eq. (4), the energy cost of this state is not the Hubbard repulsion energy U but the difference $\Delta_S = E_S - E_{++} = 2t_{\perp} - j$, which is even smaller than the orbital gap. Nevertheless, magnetic properties of these two models are similar in the limiting case (19): the longitudinal hopping generates effective atomic force microscopy longitudinal exchange $\sim t_{\parallel}^2/\Delta_S$, and the gapless spin liquid state of the resonance valence bond (RVB) type is realized.

The charge excitations exhibit more interesting character, as we discuss below. The lowest excited state is a vacancy-singlet pair occupying neighboring rungs

$$|S, i; 0, i+1\rangle = |\cdots + \sigma, i-1; S, i; 0, i+1; + \sigma, i+2 \cdots\rangle \tag{21}$$

with the energy Δ_S.

Clearly, the state $|S, i; 0, i+1\rangle$ is an analog of the charge-transfer exciton briefly discussed in the end of Sec. II. However, in this case, the exciton propagates via intermediate bonding-antibonding levels $\epsilon_{\pm}$ due to the strong inequality $t_{\perp} \gg j$. Figure 5 illustrates the mechanism of exciton propagation. Here, the rung occupied by the antibonding electron is shown by the pair of half-filled circles with filled upper half. Then the elementary hopping from doubly occupied to empty rung may be presented as

$$|S, i; 0, i+1\rangle \to |\pm, i; \mp, i+1\rangle, \tag{22}$$

and it costs the energy j, according to Eq. (11). Note that a crucial detail allowing one to discuss exciton propagation as a pure charge excitation is the fact that the spin sequence of the bonding orbitals in the initial and final states in Fig. 5 is unchanged and the spinon dispersion is unaffected by the coherent motion of the singlet exciton in the long-wave limit. This is a manifestation of the spin charge separation in quarter-filled CL model.

In the limit of extremely weak longitudinal hopping $t_{\parallel} \ll j$, the singlet-vacancy pair may propagate coherently. This pair is doubly degenerate due to its permutation symmetry, and this degeneracy manifests itself in existence of right- and

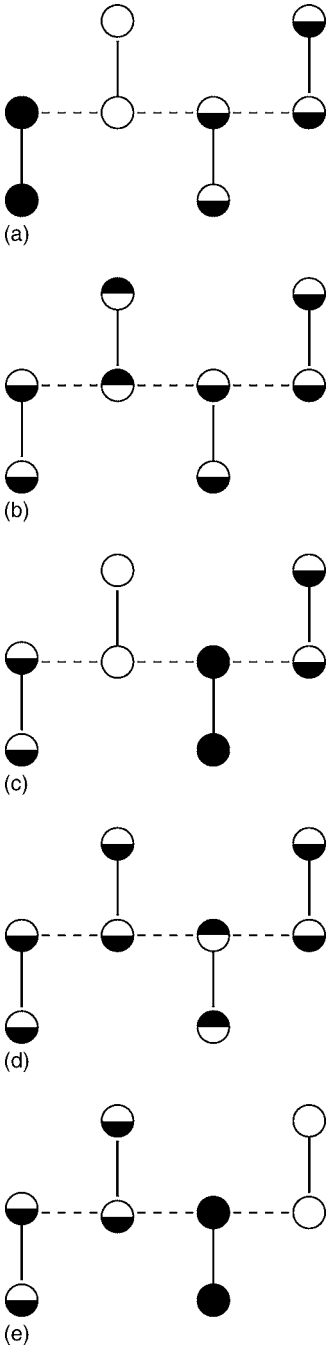

FIG. 5. Coherent motion of the vacancy-singlet exciton due to the fourth-order electron hopping $(1\rightarrow 2;2\rightarrow 3;3\rightarrow 2;4\rightarrow 3)$. Diagrams illustrate electron configurations in the initial (a), subsequent intermediate [(b)–(d)], and finite (e) states of exciton translation. Filled, empty, and half-filled (black down) and half-filled (black up) circles correspond to singlet, vacancy bonding, and antibonding electron states, respectively.

left-moving charge-transfer excitons. The fourth-order hopping process resulting in translation of the right mover between two adjacent double cells is shown in Fig. 5. Superposition of right- and left-moving excitons results in the dispersion law

$$\omega_q \sim \Delta_S - J'_{\parallel} \cos 2qa, \tag{23}$$

with $J'_{\parallel} \sim t_{\parallel}^4/j^3$. We showed before that the spin sequence remains unchanged (see Ref. 17) upon the motion of exciton, and the gain in the kinetic energy is $\sim J'_{\parallel}$. The resulting spin configuration in Fig. 5 corresponds to two spins detached from the main spin sequence on the right and attached to one on the left. For long-wave modes of exciton motion, $q\rightarrow 0$ in Eq. (23), the change in the magnetic energy associated with this disruption is negligible compared to the gain $\sim J'_{\parallel}$, and charge excitons move coherently.

Now, we turn to the case $t_{\parallel} > j$. In this situation, the coherent "vacancy-singlet" excitons are unstable against dissociation into independently propagating singlet and vacancy "defects" due to the overlap of the bands originating from the levels E_S and E_{+-}. Apparently, only incoherent propagation of such defects is possible. An example of fourth-order process resulting in decay of singlet-vacancy pair is presented in Fig. 6. Such incoherent processes will be accompanied by spin flips, antibonding-bonding deexcitation, and eventual relaxation toward the ground state.

However, coherent motion of defects is possible at small deviation from one-quarter filling. Excess holes (vacancies) behave similarly to the holes in the nearly half-filled HC in the limit (19), where the longitudinal hopping does not result in excitation of the upper orbital subband ϵ_-. In this case, one deals with a fermion gas,"fully polarized" with respect to the pseudospin τ. Excess electrons fill the side sites on the rungs without paying the Hubbard energy U, and it is easy to check that the hopping along the leg is not accompanied by creation of a spin string because the doubly occupied state is a spin singlet. As a result, the coherent propagation of these defects is also possible under the conditions (19), when the antibonding orbitals are not excited. Due to specific geometry of CL, there is no particle-hole symmetry near the 1/4 filling, and the hopping rates for particle and hole propagation are different. Direct calculation shows that the hopping rate for coherent motion of a vacancy reduces due to the kinematic constraint from $t_{\parallel}$ to $\tilde{t}_v = t_{\parallel}/2$, whereas the similar reduction for the singlets gives $\tilde{t}_s = t_{\parallel}/4$. Thus, basically the coherent motion of the vacancy and singlet can be considered in terms of tight-binding bands $\epsilon_{1,2}(k) = -2\tilde{t}_{1,2} \cos k$. Evidently, singlet (vacancy) cannot occupy the same rung twice; hence, the corresponding excitations are fermionlike. We can think of them as of spinless fermions characterized by two colors $f_{i,v}$ and $f_{i,s}$:

$$|0,i\rangle\langle +,i| \rightarrow f^{\dagger}_{i,v}, \quad |S,i\rangle\langle +,i| \rightarrow f^{\dagger}_{i,s}. \tag{24}$$

Even at exact quarter filling but at finite temperatures, the vacancies and singlets may appear at small concentrations due to thermal activation. These excitations are described by the effective two color Fermi liquid model

$$H_{eff} = \sum_{k,\alpha=v,s} \epsilon_{\alpha}(k) f^{\dagger}_{k,\alpha} f_{k,\alpha} + K \sum_{j} f^{\dagger}_{j,v} f_{j,v} f^{\dagger}_{j,s} f_{j,s}, \tag{25}$$

where the effective constant K describes effective short-range repulsion between two fermions, which prevents them from occupying the same site. This constant may be estimated as $K \sim t_{\parallel}^2/\Delta_S$, which is small compared to the band-

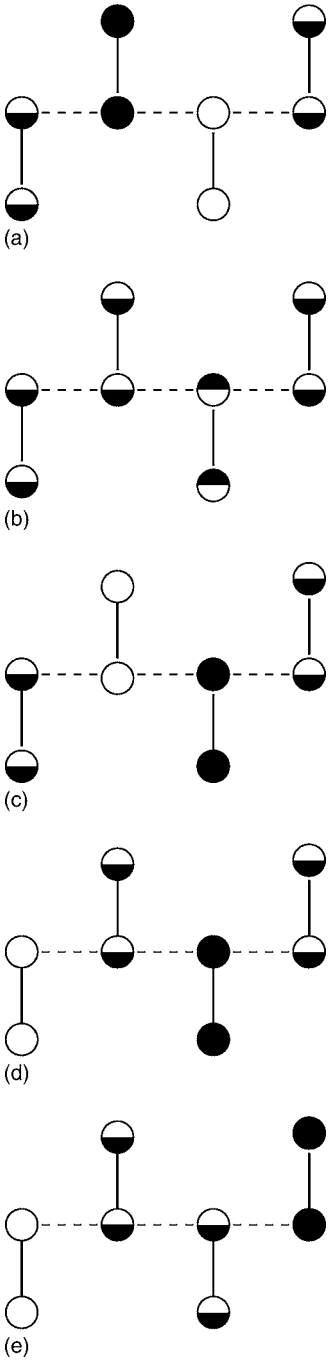

FIG. 6. Incoherent motion of the vacancy and singlet due to the fourth-order electron hopping $(2\rightarrow 3;2\rightarrow 3;1\rightarrow 2;3\rightarrow 4)$. Notations for the occupation scheme are the same as in Fig. 5.

widths $\sim t_{\parallel}$. Having in mind the asymmetric hopping Hubbard model,[18] it is tempting to analyze it using the well-established machinery of bosonization, etc. However, the sizable concentrations of vacancies and singlets are expected at temperatures comparable to the main parameter, $t_{\perp}$. This argument shows that fermion gas in H_{eff} is not degenerate, and the linearization of the spectrum around Fermi points is unjustified.

As to the excitations in the spin sector, one may say that the problem of spin excitations in the presence of a singlet or a vacancy may be mapped on the problem of RVB spin liquid with spin-one defect or dangling bond, respectively (see Ref. 19 for general approach).

To summarize, we have found, in this section, that the spin excitations are gapless Fermi-like spinons both at exact 1/4 filling and at small deviation from this point. As to the coherent charge excitations, these are gapped excitons at extremely small $t_{\parallel} \ll j$ and gapless fermions at finite doping and/or finite temperature.

IV. STRONG LONGITUDINAL HOPPING

The CL model also possesses unusual properties in the limit of strong longitudinal hopping, when it dominates over the transversal degrees of freedom:

$$t_{\parallel} \gg t_{\perp} \gg I_{\perp}. \tag{26}$$

In this case, the on-rung excitations shown in Fig. 2 are completely smeared, and the structure of low-energy spectrum of the system is predetermined by orbital degrees of freedom (bonding-antibonding subbands) and corresponding Hubbard repulsion. We will show, in this section, that in this simple situation close to the two-orbital HC, the charge excitations behave unconventionally because of the gap opening and corresponding van Hove singularities appearing in the lower partially occupied Hubbard band.

For a clear presentation, we compare the case of the asymmetric two-leg (2L) ladder and centipede ladder [see Figs. 1(b) and 1(a), respectively]. Fourier transforming along the leg, we write the kinetic part of the Hamiltonian as

$$H_{kin} = -\Psi_k^{\dagger}\begin{bmatrix} 2t_{\parallel}\cos k + \mu, & t_{\perp} \\ t_{\perp}, & 2Pt_{\parallel}\cos k - \mu \end{bmatrix}\Psi_k, \tag{27}$$

$$\Psi_k^{\dagger} = (\tilde{c}_{\alpha,k,\sigma}^{\dagger}, \tilde{c}_{\beta,k,\sigma}^{\dagger}), \tag{28}$$

where $P=1$ for the 2L model and $P=0$ for CL model. At this point, we also allow for the difference in the electrochemical potentials, $2\mu=\epsilon_{\beta}-\epsilon_{\alpha}$, between the sites α and β [see Eq. (8)]. The dispersion in these two extreme cases is given by

$$\varepsilon_{\pm}(k) = -2t_{\parallel}\cos k \mp \sqrt{\mu^2 + t_{\perp}^2}, \quad \text{2L}, \tag{29}$$

$$\varepsilon_{\pm}(k) = -t_{\parallel}\cos k \mp \sqrt{t_{\perp}^2 + (\mu + t_{\parallel}\cos k)^2}, \quad \text{CL}, \tag{30}$$

The square-root term in Eq. (29) has a meaning of effective Zeeman splitting. In contrast to 2L situation, where the $\epsilon_{+}(k)$ and $\epsilon_{-}(k)$ bands overlap, we see that in the CL case two branches of dispersion are always separated by the gap (Fig. 7). This indirect gap is given by

$$\Delta_{ind} = 2(\sqrt{t_{\perp}^2 + t_{\parallel}^2} - t_{\parallel}) \simeq t_{\perp}^2/t_{\parallel} \tag{31}$$

for the case of equal electrochemical potentials ($\mu=0$) or

$$\Delta_{ind} \simeq t_{\perp}^2 t_{\parallel}/(t_{\parallel}^2 - \mu^2) \tag{32}$$

for $\epsilon_{\alpha} \neq \epsilon_{\beta}$. The direct gap is realized at $k=\pi/2$ for $\mu=0$ and at $k=\arccos(-\mu/t_{\parallel})$, otherwise, and is equal to $\Delta=2t_{\perp}$ in

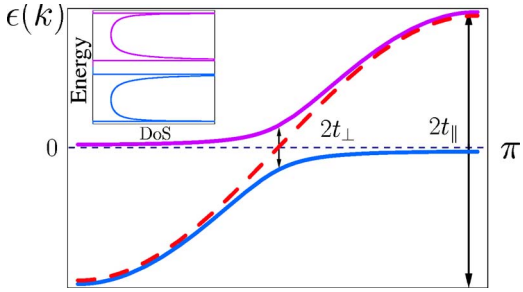

FIG. 7. (Color online) Tight-binding band structure of two lowest Hubbard subbands for quarter-filled centipede model at $t_\perp \ll t_\parallel$. The electrochemical potential $\epsilon_\alpha = \epsilon_\beta$. The direct gap corresponds old Fermi surface point $k_F = \pi/2$. The indirect gap Δ_{ind} is between the bottom of conduction band and the top of the valence band is characterized by the "flat" parts of the spectra. The inset shows the energy dependence of the density of states (DoS). The character of the DoS singularities and its influence on the response functions are discussed in the Sec. IV.

both cases. For exact 1/4 filling, the overall chemical potential $\mu_0 = \epsilon_0 = \epsilon_\alpha + \epsilon_\beta$ lies within a gap separating two bands. The existence of two (direct and indirect) gaps makes the CL case principally different from 2 L model.

One could expect that in the limit $t_\parallel \gg t_\perp$, the properties of the system will be closed to those of two-orbital Hubbard chain[14,20] because the orbital degeneracy is nearly removed by strong longitudinal hopping. This is not the case, however. The gap in the spectrum prevents formation of SU(4) manifold formed by spin and orbital degrees of freedom. However, the interband transitions as well as the edge singularities in the DoS influence the thermodynamic and optical properties of CL.

In the remainder of this section, we concentrate on the case $\mu = 0$ and consider the manifestation of singularities in the excitation spectrum in different response functions of CL. The density of states $\rho(E) = (2\pi)^{-1} \int dk \, \delta(E - \varepsilon(k))$ is divergent at $E = \pm t_\perp$ and at $E = \pm(t_\parallel + \sqrt{t_\perp^2 + t_\parallel^2})$. It behaves as

$$\rho(E) \simeq \Delta_{ind}^{-1/2} \sum_{\pm} \frac{\vartheta(-\Delta_{ind} \pm E)}{\sqrt{\pm E - \Delta_{ind}}} \tag{33}$$

at small energies $|E| \sim \Delta_{ind}$; here, $\vartheta(x) = 1$ at $x > 0$. Such character of the density of states (see inset of Fig. 7) should lead to observable anomalies in the thermodynamic quantities. The specific heat C, compressibility χ, and dc conductivity σ_{dc} are sensitive to indirect gap. Setting all fundamental constants to unity, we write for thermodynamic quantities per unit cell

$$C = \int \frac{E^2 dE}{4T^2 \cosh^2(E/2T)} \rho(E) \sim \begin{cases} \left(\frac{T}{\Delta_{ind}}\right)^{1/2}, & T \gg \Delta_{ind} \\ \left(\frac{\Delta_{ind}}{T}\right)^{3/2} e^{-\Delta_{ind}/T}, & T \ll \Delta_{ind} \end{cases} \tag{34}$$

for the specific heat and

$$\chi = \int \frac{dE}{4T \cosh^2(E/2T)} \rho(E) \sim \begin{cases} (T\Delta_{ind})^{-1/2}, & T \gg \Delta_{ind} \\ (\Delta_{ind} T)^{-1/2} e^{-\Delta_{ind}/T}, & T \ll \Delta_{ind} \end{cases} \tag{35}$$

for the compressibility along the ladder. Assuming the elastic quasiparticle lifetime τ_{el}, the dc conductivity is given by

$$\sigma_{dc} = \tau_{el} \int \frac{dk}{4T \cosh^2(\varepsilon_\pm(k)/2T)} \left(\frac{d\varepsilon_\pm(k)}{dk}\right)^2 \sim \begin{cases} \tau_{el}\sqrt{T\Delta_{ind}}, & T \gg \Delta_{ind} \\ \tau_{el}\sqrt{T\Delta_{ind}} e^{-\Delta_{ind}/T}, & T \ll \Delta_{ind}. \end{cases} \tag{36}$$

In contrast to behavior of thermodynamic quantities sensitive to indirect gap, the optical conductivity response is sensitive to direct gap. It is nonzero at $|\omega| > \Delta$ and is given by[21]

$$\sigma_{opt}(\omega) = \frac{1}{\omega} \int dk [n(\varepsilon_-(k)) - n(\varepsilon_+(k))] \times \frac{t_\perp^2 t_\parallel^2 \sin^2 k}{t_\perp^2 + t_\parallel^2 \cos^2 k} \delta(\omega + \varepsilon_-(k) - \varepsilon_+(k)) \sim \begin{cases} \frac{t_\parallel \Delta^2}{\omega^2 \sqrt{\omega^2 - \Delta^2}}, & T \ll \Delta \\ \frac{t_\parallel \Delta^2}{|\omega| T \sqrt{\omega^2 - \Delta^2}}, & T \gtrsim \Delta. \end{cases} \tag{37}$$

We, thus, see a continuous absorption band in $\sigma_{opt}(\omega)$ in contrast to the case of 2L ladder, where, as it can be easily shown (see Ref. 2), the optical conductivity consists of a single line, $\sigma_{opt}(\omega) \propto \delta(\omega \pm \Delta)$.

Interband optical transitions may result in creation of excitons with a center-of-mass momentum $Q = \pi$. Unlike the case of weak longitudinal hopping (Sec. II), these excitons arise in the conventional way due to attractive Coulomb interaction between electrons and holes. The bound electron-hole states formed on the almost flat parts of the spectrum over the indirect gap are characterized by heavy effective mass. We, therefore, expect that these excitons are nearly localized and one may neglect the processes of their coherent motion.

CONCLUSIONS AND PERSPECTIVES

In this paper, we have demonstrated several fragments of the rich phase diagram for centipede ladder. It was shown in our previous studies[12,13] that the half-filled CL is an example of spin-one chain with soft triplet-singlet excitation, which does not belong to the Haldane gap universality class. Now, we have found that the 1/4 filled CL also demonstrates unconventional properties both in spin and charge sectors.

We considered here only three limiting cases of the quarter-filled CL, where the character of charge and spin excitations may be revealed by means of relatively simple arguments. First, we have found the regime where CL behaves as a spin-one chain with ferromagnetic effective longitudinal exchange and magnonlike excitation spectrum (Sec. II). It is shown that the system is unstable against dimerization at strong enough on-rung ferromagnetic exchange. The only coherent mode in the charge sector is the gapped triplet charge-transfer exciton.

One should stress that the dimerization effect offered in this section has no analogs in current literature. Usually the dimerization mechanism in spin chains is either explicitly built in the Heisenberg Hamiltonian or arises as a result of competition between the nearest and next nearest exchange coupling.[22] As to the two-leg ladders, the dimerized configurations were considered in a context of RVB states (rung-dimer states versus leg-dimer states).[23] In our case, the lattice period is doubled as a result of competition between the *on-rung* hopping and exchange coupling. Experimentally, rung dimerization as a result of charge redistribution between legs and rungs was detected optically[7] in two-leg compounds AV_6O_{15} (A=Na, Sr). However, in vanadium bronzes, this effect is driven mainly by the valence instability of V ions.

Second, we have described the situation, where the vacancies (empty rungs) and spin singlets (doubly occupied rungs) may propagate either as coherent excitons or as independent spinless fermionic quasiparticles with different Fermi velocities (Sec. III). The dispersion law is gapped in the former case and gapless in the second case, where the charge sector may be described as a two-component Fermi liquid with weak short-range interaction. The spin subsystem behaves as the RVB-type spin liquid, where the spinons propagate in the presence of spin-one and dangling bond defects.

Third, we have considered the limit of strong longitudinal hopping, where the CL behaves as a specific version of two-orbital Hubbard chain. The peculiar features of this limit are the appearance of a gap in the half-occupied lower Hubbard band. This gap has purely hybridization nature, but the van Hove singularities in the density of states strongly influence the thermodynamic and optical properties of CL.

Our analysis of these three cases by no means exhausts the variety of unusual properties of CL at partial filling. In particular, we did not include in our Hamiltonian direct longitudinal exchange, which can enhance the indirect kinetic exchange or compete with it. We did not consider the phase transitions between different phases, which may have their own peculiarities as compared to currently studied quantum phase transitions in low-dimensional systems.[24] We also did not discuss possible lattice distortions, which may accompany dimerization. All these and many other open questions are left for future investigation.

The centipede ladder shown in Fig. 1 is the simplest example of the family of quasi-1D systems intermediate between chains and two-leg ladders. The experimental realization of such system [organic biradical crystals PNNNO (Ref. 11)] is already known, but one may easily imagine molecular chains decorated not with rungs but with radicals forming closed loops, zigzags, etc. We believe that the study of excitation spectra, and magnetic and transport properties of this family will bring unexpected results.

ACKNOWLEDGMENTS

We are grateful to F. Assaad, B. N. Narozhny, and A. M. Tsvelik for useful and stimulating discussions. D.N.A. thanks ICTP for the hospitality. M.N.K. appreciates support from the Heisenberg program of the DFG and the SFB-410 research grant during initial stage of the CL project. This work was supported (M.N.K.) by the U.S. Department of Energy Office of Science through Contract No. DE-AC02-06CH11357.

APPENDIX: CALCULATION OF THE SUPEREXCHANGE INTERACTION

In order to calculate $J_\parallel$, we note that two spins $S=1$ at even sites in Eq. (17) and in Fig. 3 can be combined into total spin $S_{tot}=0,1,2$. The scalar product $\mathbf{S}_i\cdot\mathbf{S}_{i+2}=\frac{1}{2}((\mathbf{S}_i+\mathbf{S}_{i+2})^2-\mathbf{S}_i^2-\mathbf{S}_{i+2}^2)$ in Eq. (16) attains values $-2,-1,1$ for these values S_{tot}, respectively. The value of $3J_\parallel$ can, hence, be naively calculated as a difference in fourth-order corrections (15) to the states $S_{tot}=0$ and $S_{tot}=2$.

Let us use a shorthand notation $|m,m'\rangle$ for a quantum state $|Tm,i;Tm',i+2\rangle$, and $\Phi_{L,m}$ for the state with total spin $S_{tot}=L$ and its z-component m. The weight of $\Phi_{L,m''}$ in $|m,m'\rangle$ is the Clebsch-Gordan coefficient $C^{Lm''}_{1m1m'}$. Then the states we are interested in, $S_{tot}=0$ and $S_{tot}=2$, are given by $\Phi_{0,0}=(|-1,1\rangle+|1,-1\rangle-|0,0\rangle)/\sqrt{3}$ and $\Phi_{2,2}|1,1\rangle$.

Further, we denote the combinations $|+\sigma_1,i;+\sigma_3,i+2\rangle$ in $|\phi^{(2)}\rangle$, Eq. (16), as "nonlocal triplet" states, e.g., $|+\uparrow,i;+\uparrow,i+2\rangle=|\tilde{T}1,i+1\rangle$, etc. The intermediate state in Fig. 3, obtained after two longitudinal hops in terms of its spin components, is rather obviously classified in the same terms of total spin, composed of two triplets, $|Tm,i+1\rangle$ and $|\tilde{Tm},i+1\rangle$. Similarly denoting $|\tilde{Tm},i+1;Tm',i+1\rangle=|m,\tilde{m}'\rangle$, we have $\tilde{\Phi}_{0,0}=(|-\tilde{1},1\rangle+|1,\tilde{-1}\rangle-|0,\tilde{0}\rangle)/\sqrt{3}$, etc.

It then can be shown that (projecting at each step at the states with lowest energy, bonding and triplet, as discussed above)

$$\mathcal{H}_l^2|-1,1\rangle=\frac{t_\parallel^2}{2\sqrt{2}}|+\downarrow,i;T0,i+1;+\uparrow,i+2\rangle,$$

$$\mathcal{H}_l^2(|-1,1\rangle+|1,-1\rangle)=\frac{t_\parallel^2}{2}\widetilde{|0,0\rangle}=\frac{t_\parallel^2}{2}\left[\sqrt{\frac{2}{3}}\tilde{\Phi}_{2,0}-\sqrt{\frac{1}{3}}\tilde{\Phi}_{0,0}\right],$$

$$\mathcal{H}_l^2|0,0\rangle=\frac{t_\parallel^2}{4}(\widetilde{|-1,1\rangle}+\widetilde{|1,-1\rangle}+\widetilde{|0,0\rangle})=\frac{t_\parallel^2}{4}\left[2\sqrt{\frac{2}{3}}\tilde{\Phi}_{2,0}+\sqrt{\frac{1}{3}}\tilde{\Phi}_{0,0}\right], \quad \text{(A1)}$$

which leads to $\mathcal{H}_l^2\Phi_{0,0}=-\frac{t_\parallel^2}{4}\tilde{\Phi}_{0,0}$. Similarly, one obtains $\mathcal{H}_l^2\Phi_{2,2}=\frac{t_\parallel^2}{2}\tilde{\Phi}_{2,2}$. Because the projected action of $\mathcal{H}_l^2$ is self-conjugate, we obtain $\mathcal{H}_l^4\Phi_{0,0}=\frac{t_\parallel^4}{16}\Phi_{0,0}$ and $\mathcal{H}_l^4\Phi_{2,2}=\frac{t_\parallel^4}{4}\Phi_{2,2}$.

We would also like to exclude more complex structure of the effective Hamiltonian, namely,

$$\mathcal{H}_{eff} = -J_{\parallel}\sum_i (\mathbf{S}_i \cdot \mathbf{S}_{i+2} + c_1(\mathbf{S}_i \cdot \mathbf{S}_{i+2})^2), \qquad \text{(A2)}$$

which is not prohibited by symmetry.

To this end, we calculate also the correction to states $\Phi_{1,m}$ of total spin $L=1$. Within the same logic, we have $\mathcal{H}_l^2(|1,-1\rangle - |-1,1\rangle) = \mathcal{H}_l^2\sqrt{2}\Phi_{1,0} = \frac{t_\parallel^2}{2}|\tilde{S},i+1;T0,i+1\rangle$, where $\tilde{S}$ nonlocal singlet. Therefore, $\mathcal{H}_l^4\Phi_{1,0} = \frac{1}{8}t_\parallel^4\Phi_{1,0}$ and for our values $L=0,1,2$, we have the corrections $-1/16,-1/8,-1/4$ in units of $t_\parallel^4/\Delta_T^3$, respectively. It means that $J_\parallel = t_\parallel^4/(16\Delta_T^3)$ and $c_1=0$. Thus, the anisotropy term $(\mathbf{S}_i\cdot\mathbf{S}_{i+2})^2$ does not appear in the fourth-order of longitudinal hopping. The reason of it is very simple: in order to get the four-spin $S=1$ interaction within the scheme shown on Fig. 3 where four spins $s=1/2$ participate, one needs at least eight processes of longitudinal hopping.

*On leave from Petersburg Nuclear Physics Institute, Gatchina 188300, Russia.

[1] E. Dagotto and T. M. Rice, Science **271**, 618 (1996).

[2] A. O. Gogolin, A. A. Nersesyan, and A. M. Tsvelik, *Bosonization and Strongly Correlated Systems* (Cambridge University Press, Cambridge, 1998).

[3] F. H. L. Essler, H. Frahm, F. Göhmann, A. Klümper, and V. E. Korepin, *The One-Dimensional Hubbard Model* (Cambridge University Press, Cambridge, 2005).

[4] T. Giamarchi, *Quantum Physics in One Dimension* (Clarendon, Oxford, 2004).

[5] D. G. Shelton, A. A. Nersesyan, and A. M. Tsvelik, Phys. Rev. B **53**, 8521 (1996).

[6] D. Controzzi and A. M. Tsvelik, Phys. Rev. B **72**, 035110 (2005).

[7] V. T. Phuoc, C. Sellier, and E. Janod, Phys. Rev. B **72**, 035120 (2005).

[8] F. H. L. Essler and A. M. Tsvelik, Phys. Rev. Lett. **88**, 096403 (2002).

[9] B. N. Narozhny, S. T. Carr, and A. A. Nersesyan, Phys. Rev. B **71**, 161101(R) (2005); S. T. Carr, B. N. Narozhny, and A. A. Nersesyan, *ibid.* **73**, 195114 (2006).

[10] H. J. Schulz, Phys. Rev. Lett. **64**, 2831 (1990).

[11] Y. Hosokoshi, Y. Nakazawa, K. Inoue, K. Takizawa, H. Nakano, M. Takahashi, and T. Goto, Phys. Rev. B **60**, 12924 (1999).

[12] M. N. Kiselev, D. N. Aristov, and K. Kikoin. Phys. Rev. B **71**, 092404 (2005).

[13] M. N. Kiselev, D. N. Aristov, and K. Kikoin, Physica B **359-361**, 1406 (2005).

[14] Y. Yamashita, N. Shibata, and K. Ueda, Phys. Rev. B **58**, 9114 (1998).

[15] K. Kikoin and Y. Avishai, Phys. Rev. Lett. **86**, 2090 (2001); Phys. Rev. B **65**, 115329 (2002).

[16] M. Takahashi, Prog. Theor. Phys. **87**, 233 (1986).

[17] D. N. Aristov and D. R. Grempel, Phys. Rev. B **55**, 11358 (1997).

[18] J. K. Freericks, E. H. Lieb, and D. Ueltschi, Phys. Rev. Lett. **88**, 106401 (2002).

[19] S. Eggert and I. Affleck, Phys. Rev. B **46**, 10866 (1992).

[20] V. L. Pokrovskii and G. V. Uimin, Zh. Eksp. Teor. Fiz. Pis'ma Red. **11**, 206 (1970); G. V. Uimin, Zh. Eksp. Teor. Fiz. Pis'ma Red. **12**, 322 (1970); [JETP Lett. **12**, 225 (1970)].

[21] D. N. Aristov and R. Zeyher, Phys. Rev. B **70**, 212511 (2004); **72**, 115118 (2005).

[22] H.-J. Mikeska and A. K. Kolezhuk, *One-Dimensional Magnetism*, Lecture Notes in Physics Vol. 645, (Springer-Verlag, Berlin, 2004), pp. 1–83.

[23] M. Nakamura, T. Yamamoto, and K. Ida, J. Phys. Soc. Jpn. **72**, 1022 (2003).

[24] S. Sachdev, *Quantum Phase Transitions* (Cambridge University Press, Cambridge, 1999); *Quantum Phases and Phase Transitions of Mott Insulators*, Lecture Notes in Physics Vol. 645 (Springer-Verlag, Berlin, 2004) pp. 381–432.